Cell Death and Differentiation (2008) 15, 1499–1509
© 2008 Nature Publishing Group All rights reserved 1350-9047/08 $30.00
www.nature.com/cdd

The co-translocation of ERp57 and calreticulin determines the immunogenicity of cell death

T Panaretakis[1,2,3,10], N Joza[1,2,3,10], N Modjtahedi[1,2,3], A Tesniere[1,2,3], I Vitale[1,2,3], M Durchschlag[4], GM Fimia[5], O Kepp[1,2,3], M Piacentini[5,6], K-U Froehlich[4], P van Endert[7,8], L Zitvogel[2,3,9], F Madeo[4] and G Kroemer*[,1,2,3]

The exposure of calreticulin (CRT) on the plasma membrane can precede anthracycline-induced apoptosis and is required for cell death to be perceived as immunogenic. Mass spectroscopy, immunofluorescence and immunoprecipitation experiments revealed that CRT co-translocates to the surface with another endoplasmic reticulum-sessile protein, the disulfide isomerase ERp57. The knockout and knockdown of CRT or ERp57 inhibited the anthracycline-induced translocation of ERp57 or CRT, respectively. CRT point mutants that fail to interact with ERp57 were unable to restore ERp57 translocation upon transfection into *crt*$^{-/-}$ cells, underscoring that a direct interaction between CRT and ERp57 is strictly required for their co-translocation to the surface. ERp57^{low} tumor cells generated by retroviral introduction of an ERp57-specific shRNA exhibited a normal apoptotic response to anthracyclines *in vitro*, yet were resistant to anthracycline treatment *in vivo*. Moreover, ERp57^{low} cancer cells (which failed to expose CRT) treated with anthracyclines were unable to elicit an anti-tumor response in conditions in which control cells were highly immunogenic. The failure of ERp57^{low} cells to elicit immune responses and to respond to chemotherapy could be overcome by exogenous supply of recombinant CRT protein. These results indicate that tumors that possess an intrinsic defect in the CRT-translocating machinery become resistant to anthracycline chemotherapy due to their incapacity to elicit an anti-cancer immune response.

Cell Death and Differentiation (2008) **15,** 1499–1509; doi:10.1038/cdd.2008.67; published online 9 May 2008

The conventional treatment of cancer relies upon radiotherapy and chemotherapy, two procedures that supposedly mediate their therapeutic effects solely by intrinsic mechanisms of tumor cell death and without direct participation by the host immune system. Nevertheless, there are specific circumstances in which conventional anti-cancer treatments can induce a modality of cell death that is immunogenic, whereby dying cells elicit a tumor-specific immune response culminating in elimination of tumor cells. Although most chemotherapeutic agents kill tumor cells through a morphologically indistinguishable apoptotic pathway, they differ in their capacity to stimulate immunogenic as opposed to non-immunogenic cell death.[1] Recently, we reported that tumor cells undergoing immunogenic cell death translocate intracellular calreticulin (endo-CRT) to their plasma membrane (PM) surface (ecto-CRT), facilitating tumor cell recognition and engulfment by dendritic cells (DC) and subsequent T-cell-mediated elimination of the tumor.[2] Accordingly, anthracyclines and γ-irradiation, which elicit immunogenic cell death, induce CRT exposure whereas other proapoptotic agents that induce non-immunogenic cell death fail to induce ecto-CRT.[2–4] Depletion of CRT abolishes the immunogenicity of cell death elicited by anthracyclines, whereas addition of exogenous CRT or enforced surface exposure of CRT by pharmacological agents that favor CRT translocation can enhance the immunogenicity of cell death.[2,4]

An additional signal emitted during immunogenic cell death is the release of the nuclear protein HMGB1 into the extracellular space.[5] Subsequent interaction of HMGB1 with toll-like receptor (TLR)4 expressed on DC drives optimal antigen presentation by DC.[6] Knockout of TLR4 or its downstream effector MyD88 (in mice), or loss-of-function mutations of TLR4 that disrupt its binding to HMGB1 (such as the Gly299Asn substitution in humans), abolishes the capacity of DC to present antigen from apoptotic tumor cells *in vitro* and *in vivo*. Importantly, TLR4 mutations also affect the propensity of breast cancer patients to relapse after immunogenic anti-cancer therapy (with anthracyclines or localized radiotherapy), thus providing the first molecular epidemiological evidence that the immune system actually contributes to the efficacy of anti-cancer chemotherapy in humans.[5,7]

CRT is a Ca^{2+}-binding protein with two sites (with high and low capacity) for buffering Ca^{2+}, thus affecting Ca^{2+} signaling and Ca^{2+} homeostasis.[8–10] CRT is a soluble protein

[1]INSERM, Unit 848 'Apoptosis, Cancer and Immunity', F-94805 Villejuif, France; [2]Institut Gustave Roussy, F-94805 Villejuif, France; [3]Faculté Paris Sud-Université Paris 11, F-94805 Villejuif, France; [4]Institute of Molecular Biosciences, Universitaetsplatz 2, University of Graz, 8010 Graz, Austria; [5]National Institute for Infectious Diseases 'Lazzaro Spallanzani', 00149 Rome, Italy; [6]Department of Biology, University of Rome 'Tor Vergata', 00173 Rome, Italy; [7]INSERM, U580, F-75015 Paris, France; [8]Faculté de Médecine René Descartes, Université Paris-Descartes, F-75015 Paris, France and [9]INSERM, U805, Institut Gustave Roussy, F-94805 Villejuif, France
*Corresponding author: G Kroemer, INSERM, U848, Institut Gustave Roussy, PR1, 39, rue Camille Desmoulins, F-94805 Villejuif, France.
Tel: +33 1 42 11 60 46; Fax: 33 1 42 11 60 47; E-mail: kroemer@igr.fr
[10]These authors contributed equally to this work.
Keywords: apoptosis; endoplasmic reticulum; anthracyclines
Abbreviations: Bac, bacitracin; CRT, calreticulin; DAPI, 4′,6-diamidino-2-phenylindole; DC, dendritic cells; ER, endoplasmic reticulum; FBS, fetal bovine serum; MHC, major histocompatibility complex; PBS, phosphate-buffered saline; PDI, protein disulfide isomerases; PFA, paraformaldehyde; PI, propidium iodide; PM, plasma membrane; rec.CRT, recombinant calreticulin; recERp57, recombinant ERp57
Received 31.1.08; revised 17.3.08; accepted 31.3.08; Edited by P Bouillet; published online 9.5.08

that is mainly located in the lumen of the endoplasmic reticulum (ER) where it also functions as a chaperone and a lectin interacting with several proteins endowed with disulfide isomerase activity, in particular ERp57.[11,12] A fraction of CRT resides outside of the ER, where it has been suggested to regulate nuclear protein transport,[13] signaling via nuclear steroid receptors[14] and integrin signaling.[9] CRT consists of a globular amino-terminal N-domain, which is involved in carbohydrate binding; a central P-domain, which is folded in an 'extended arm' and interacts with ERp57; and an acidic carboxy-terminal C-domain, which binds Ca^{2+}. The mechanisms through which CRT translocates to the PM surface are not known, although they involve caspase activation, an ER stress response leading to the phosphorylation of the eukaryotic initiation factor eIF2α, and active exocytosis.[1,15,16] The exact structure to which CRT binds on the surface is unknown, although it is plausible, based on its lectin activity, that it binds to carbohydrates of the glycocalix. The receptor of CRT on DC is also elusive, yet it might include scavenger receptor A, scavenger receptor expressed by endothelial cell-I,[17] CD91[18] or many other molecules such as CD40 ligand, TRAIL and Fas ligand.[19]

ERp57, which tightly binds to CRT in the ER lumen,[11] catalyzes disulfide oxidation, isomerization and reduction of native glycoproteins. ERp57 is also an integral component of the peptide-loading complex of the major histocompatibility complex (MHC) class I pathway.[20,21] Similar to other protein disulfide isomerases (PDI), ERp57 comprises two thioredoxin-like catalytic domains located in the amino and carboxyl termini, separated by two non-catalytic domains that bind the substrate.[22,23] The lack of ERp57 expression constitutes a negative prognostic marker in some neoplasias, for instance in human gastric cancer.[24] The potential of PDI family members, including ERp57, to translocate to the cell surface has been reported.[25,26]

Here, we report that ERp57 and CRT co-translocate from the ER lumen to the PM surface after treatment of cancer cells with anthracyclines. This discovery allowed us to manipulate the translocation of CRT to the surface indirectly, via knocking down of ERp57, and to construct tumor cell lines that fail to expose CRT after anthracycline treatment. We provide evidence for a new type of chemotherapy resistance due to the inability of cancer cells to expose CRT to the cell surface, leading to the failure of tumor cell death to elicit an immune response.

Results and Discussion

Early translocation of ERp57 to the surface of anthracycline-treated tumor cells. CT26 colon cancer cells were left untreated (control) or were treated with the anthracycline mitoxantrone (MTX) for 4 h, followed by biotinylation of PM proteins, purification of such biotinylated proteins on a streptavidin column and two-dimensional gel electrophoresis.[2] This procedure led to the mass spectroscopic identification of spots that were more abundant (by a factor of $\geqslant 3$) after anthracycline treatment. One series of four spots (arrow and arrowheads in Figure 1a) with an identical molecular mass of $\sim$55 kDa and distinct isoelectric points (which presumably reflect variable degrees of phosphorylation) was identified as ERp57 (Figure 1b). Indeed, immunofluorescence staining of CT26 cells revealed that MTX treatment induced translocation of ERp57 to the cell surface (ecto-ERp57) (Figure 1c) to a similar level (Figure 1d) and with similar kinetics (Figure 1e) as CRT (ecto-CRT), well before the cells stained positively for the early apoptotic marker annexin V (Figure 1f). These data, which could be recapitulated in mouse embryonic fibroblasts (see below) and HeLa cells (Supplementary Figure 1), indicate that ERp57 exposure, like CRT exposure,[2] occurs at a pre-apoptotic stage, shortly after anthracycline treatment.

Co-translocation of ERp57 and CRT to the cell surface. Irradiation with UVC light, another stimulus for inducing ecto-CRT,[3] also led to the appearance of ERp57 on the cell surface (Figure 2a). Two-color surface immunofluorescence detection of ecto-ERp57 and ecto-CRT, followed by cytofluorometry, revealed a strong correlation between ecto-ERp57 and ecto-CRT exposure to the cell surface (Figure 2a). In addition, immunofluorescence staining, followed by confocal microscopy, revealed that after MTX treatment both ERp57 and CRT co-localized at discrete foci on the PM surface (Figure 2b). Ecto-CRT largely co-localized with PM microdomains (Supplementary Figure 2), explaining its patchy distribution. Immunoprecipitation experiments performed on biotinylated surface proteins also revealed that ecto-CRT co-immunoprecipitated with ecto-ERp57 (Figure 2c). Remarkably, the co-translocation of CRT and ERp57 was phylogenetically conserved. Yeast (*Saccharomyces cerevisiae*) cells manipulated to express a GFP-labeled CRT ortholog (cne1p) and a YFP-labeled ERp57 ortholog (pdi1p) also exhibited the co-translocation of both proteins to discrete foci on the cell surface following culture with MTX (Figure 2d). Altogether, these results indicate that ERp57 and CRT traffic together to the PM surface.

CRT is required for ERp57 cell surface exposure. Mouse embryonic fibroblasts (MEF) that carry a homozygous null mutation in CRT ($crt^{-/-}$) failed to expose ERp57 in response to MTX, although they contain normal amounts of ERp57[27] (Figure 3a and b). Similarly, CT26 cells subjected to CRT knockdown with a small-interfering RNA (Figure 3c), a manipulation that did not affect the expression level of MHC class I molecules (Figure 3d), failed to expose ERp57 on the surface after MTX or UVC treatment (Figure 3e). Transfection of $crt^{-/-}$ MEF with a *crt*-expressing plasmid restored their ability to expose ERp57 in response to MTX. However, point mutations that affect the capacity of CRT to physically interact with ERp57 (W244 and D241)[28] abolished ERp57 exposure (Figure 3f and g). In yeast, the knockout of the CRT ortholog (Δcne1) greatly reduced surface exposure of the ERP57 ortholog (pdi1 fused to GFP) following MTX treatment, underscoring the phylogenetic conservation of the obligate co-translocation of ERp57 and CRT (Figure 3h and i).

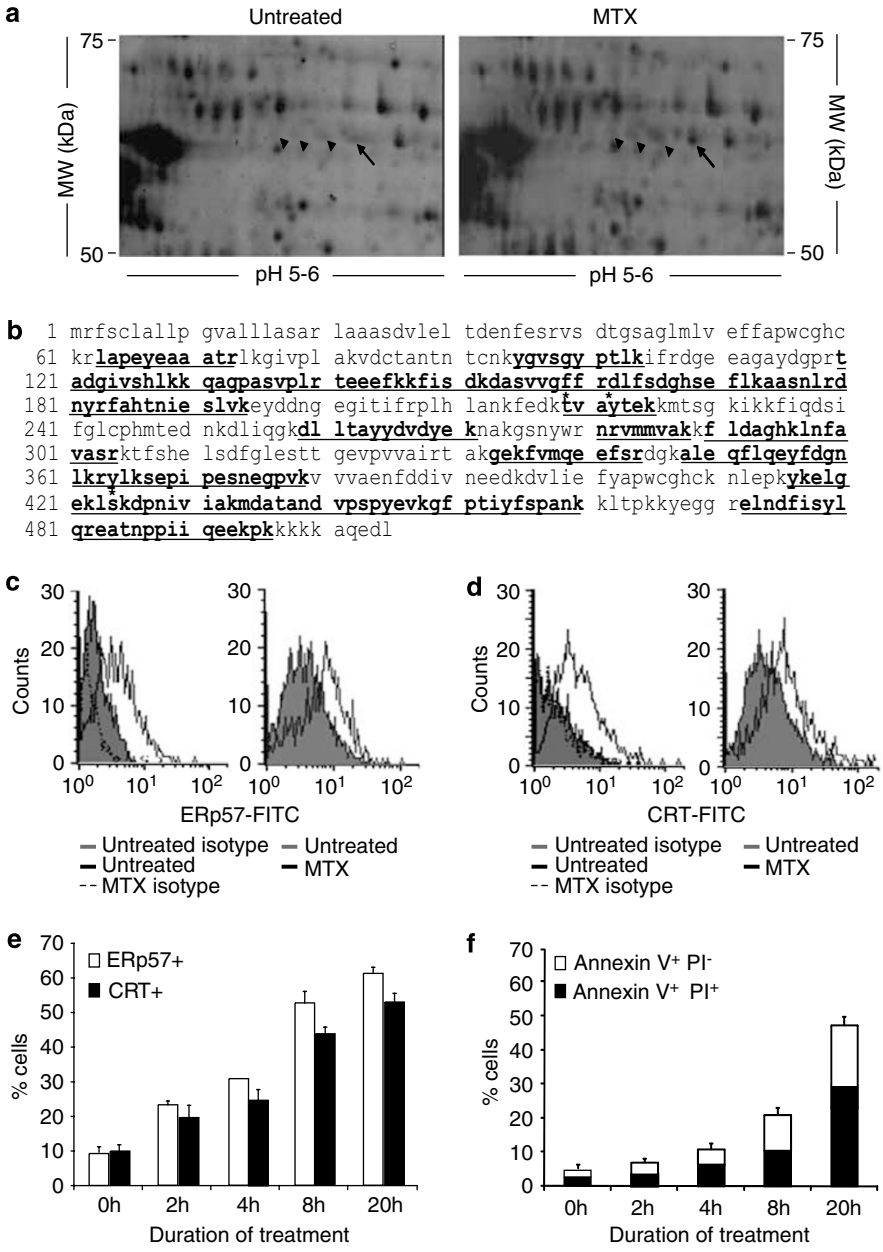

Figure 1 Cell surface exposure of ERp57 induced by MTX. (**a**) Identification of ERp57 as a protein that is exposed on the cell surface upon treatment with MTX. CT26 cells were treated for 4 h with MTX, followed by purification of the biotinylated PM proteins and two-dimensional gel electrophoresis. The arrow indicates the MTX-induced spot identified as ERp57 and the arrowheads point to the spots identified as the phosphorylated forms of ERp57. (**b**) The indicated peptide sequences (bold and underlined) were identified by mass spectrometry to correspond to the ERp57 sequence. The asterisks indicate phosphorylated amino acids identified by mass spectroscopy. The cell surface exposure of ERp57 was determined by immunofluorescence cytometry among viable (propidium iodide (PI)-negative) cells as described in Materials and Methods. (**c**) Untreated control or MTX-treated CT26 cells stained with an isotype control or an anti-ERp57 antibody after 4 h of treatment. (**d**) Untreated control or MTX-treated CT26 cells stained with an isotype control or an anti-CRT antibody after 4 h of treatment followed by immunofluorescence cytometry. (**e**) Kinetics of ERp57 and CRT surface exposure determined by FACS analysis after incubation of CT26 cells with MTX. Results are the means ± S.E.M. of three experiments. (**f**) Quantitative analysis of annexin V-FITC and PI staining of CT26 cells treated with 1 μM MTX for the indicated time points. Results are the means ± S.E.M. of three experiments

ERp57 is required for CRT cell surface exposure. In contrast to wild-type (WT) MEF, *erp57*$^{-/-}$ MEF failed to expose CRT when treated with MTX (Figure 4a and b). We generated CT26 cell clones stably expressing shRNA specific for ERp57 (ERp57^{low}); knockdown of ERp57 was confirmed by western blotting (Figure 4c). The stable knockdown of ERp57 (Figure 4c) was accompanied by the reduced expression of MHC class I molecules on the cell surface (Figure 4d) and also led to a defective CRT exposure after MTX or UVC treatment (Figure 4e). Re-expression of *erp57* into *erp57*$^{-/-}$ MEF (Figure 5a) restored MHC class I expression (Figure 5b) and CRT exposure in response to

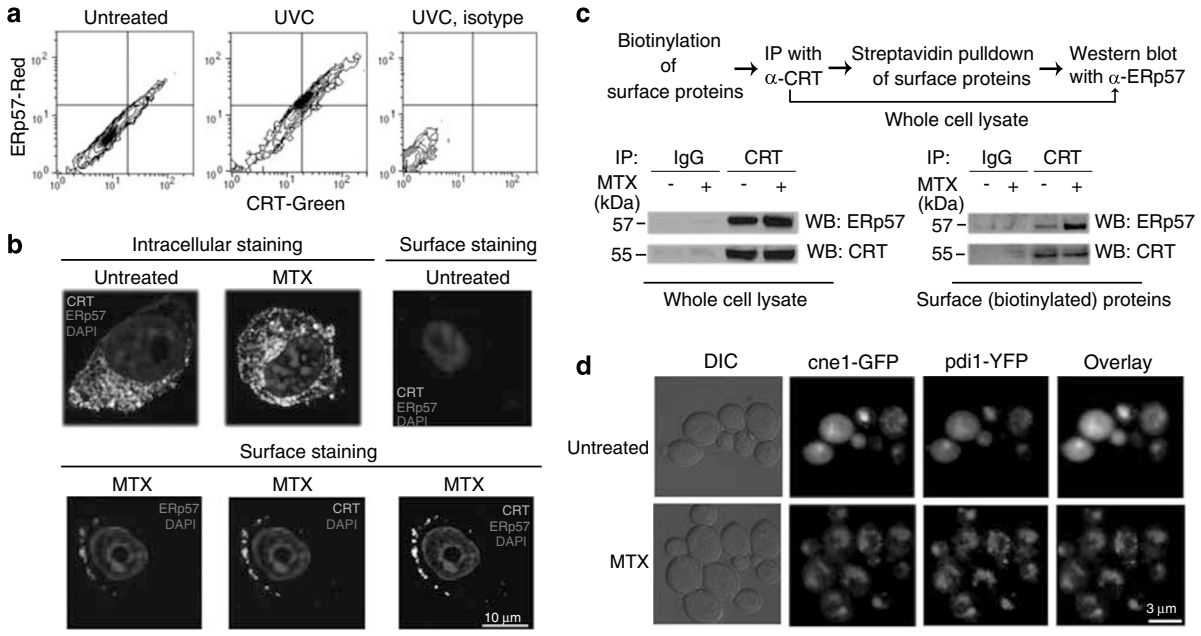

Figure 2 ERp57 and CRT co-translocate to the cell surface. (**a**) The simultaneous cell surface exposure of CRT and ERp57 in CT26 cells irradiated with UVC light (100 J/cm^2) was determined by immunofluorescence cytometry among viable (4′,6-diamidino-2-phenylindole (DAPI)-negative) cells. Four hours after UVC treatment, CT26 cells were stained with anti-ERp57 (red) and anti-CRT (green) antibodies. Untreated and treated cells were stained 4 h after treatment. (**b**) Immunofluorescence detection of CRT (appearing in green, FITC) and ERp57 (red, Alexa 568) within the cell (after fixation and permeabilization) and on the cell surface (in non-permeabilized cells) after treatment of cells with MTX for 2 h. The nuclei were visualized with DAPI. (**c**) Schematic representation of the protocol used to immunoprecipitate surface CRT and ERp57. Whole-cell lysates and isolated cell surface proteins were immunoprecipitated with anti-CRT (or as a control an unrelated IgG) and the western blots were probed with anti-ERp57 and anti-CRT. (**d**) *S. cerevisiae* cells expressing Cne1-GFP and Pdi1p-YFP were untreated or treated with MTX for 4 h. The yeast cells were visualized by phase-contrast (DIC) and fluorescent microscopy as described in Materials and Methods

MTX (Figure 5c). The fact that *erp57*$^{-/-}$ MEF manifest a similar defect in CRT exposure as cells transfected with an ERp57-secific shRNA suggests that the phenotype induced by shRNA is not due to an off-target effect. Expression of an ERp57 mutant that lost its disulfide isomerase activity[23] failed to restore MHC class I expression (Figure 5b), but was able to rescue CRT exposure (Figure 5c). These findings indicate that ERp57 (but not its disulfide isomerase activity) is required for CRT exposure. Accordingly, we found that disulfide isomerase chemical inhibitors (phenylarsine oxide, 5,5-dithiobis-(2-nitrobenzoic acid) and bacitracin (Bac)) were unable to inhibit the surface exposure of CRT and ERp57 in anthracycline-treated tumor cells (as exemplified for Bac in Supplementary Figure 3). Thus, the physical interaction between ERp57 and CRT is required for their co-translocation to the PM surface, yet the disulfide isomerase activity of ERp57 is dispensable for this process.

Exogenous CRT restores the deficient immunogenic response of ERp57^{low} cells *in vivo*. ERp57^{low} CT26 cells have low MHC class I expression (see above; Figure 4d) and are deficient in MTX-induced CRT exposure. As expected, ERp57^{low} CT26 cells treated with MTX were far less efficient in eliciting an anti-tumor immune response than control CT26 cells used in identical conditions. This was monitored by inoculating live CT26 control cells into mice that had been injected with MTX-treated tumor cells (either control in Figure 6a or ERp57^{low} in Figure 6b) 1 week before, in the absence of any adjuvant. Recombinant CRT could be adsorbed to untreated or MTX-treated ERp57^{low} cells, exactly with the same efficacy as to control cells (Figure 6d). In contrast, recombinant ERp57 (recERp57) was not absorbed by either control (Figure 6e) or ERp57^{low} (not shown) CT26 cells. Addition of endotoxin-free recombinant CRT (rec.CRT) protein fully restored the immunogenicity of MTX-treated ERp57^{low} CT26 cells (Figure 6c), indicating that lack of CRT exposure (rather than lack of class I exposure) explains the deficient immunogenicity of MTX-treated ERp57^{low} CT26 cells.

ERp57 has no effect on the mitoxantrone response *in vitro* but dictates chemotherapy responses *in vivo*. *In vitro*, ERp57^{low} CT26 cells responded to MTX in a similar manner to control (shRNA scrambled) CT26 cells. Thus, ERp57^{low} and control cells underwent similar levels of apoptosis in short-term assays (48 h) with an IC_{50} of $\sim$0.5 μM (Figure 7a) and a similar reduction in clonogenic survival in long-term assays (2 weeks) with an IC_{50} of $\sim$20 nM (Figure 7b). In strict contrast, the *in vivo* response of ERp57^{low} CT26 to MTX was reduced. Control and ERp57^{low} CT26 tumors grew with a similar kinetics after their subcutaneous inoculation into immunocompetent, isogenic BALB/c mice (upper panels in Figure 7c). However, after intratumoral MTX injection, only mice injected with control CT26 cells eliminated their tumors. Most (4 out of 5) mice injected with ERp57^{low} CT26 cells failed to respond to MTX and eliminate their tumors, in an experimental setting in which anti-tumor immune responses dictate the efficacy of

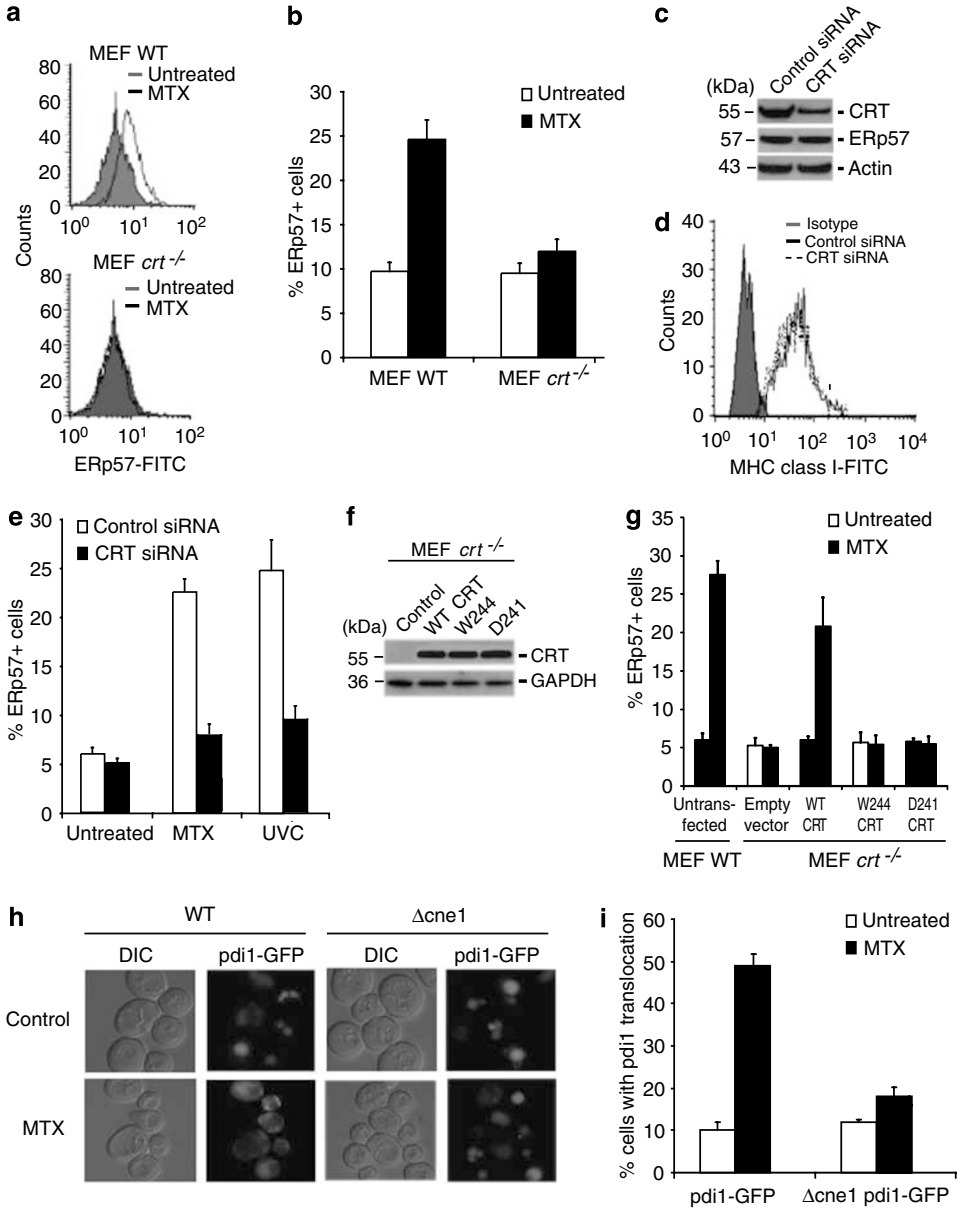

Figure 3 CRT is required for the translocation of ERp57 to the cell surface. (**a**) WT and *crt*$^{-/-}$ MEF were treated with MTX for 2 h and analyzed for ERp57 exposure by cytofluorimetric immunodetection. (**b**) Quantitative analysis of cells with surface ERp57 after incubation of WT and *crt*$^{-/-}$ MEF with MTX. Data are the means ± S.E.M. of three independent experiments. (**c**) CT26 cells were transfected with siRNA specific for CRT followed by immunoblot detection of CRT and ERp57. Actin was used as a loading control. (**d**) Cell surface immunofluorescent detection of MHC class I in live CT26 cells transfected with either control siRNA or CRT siRNA. (**e**) Quantitative analysis of CT26 cells with surface ERp57 transfected with either control siRNA or CRT siRNA and treated with the indicated agents. (**f**) Immunoblot analysis of *crt*$^{-/-}$ MEF transfected with either an empty vector or the following HA-tagged CRT constructs: WT-CRT, W244-CRT, D241-CRT. The expressed CRT constructs were visualized with anti-HA and anti-CRT antibodies. GAPDH was used as a loading control. (**g**) Quantitative analysis of cells with surface ERp57 after transfection of *crt*$^{-/-}$ MEF with the indicated constructs and treatment with MTX for 2 h. (**h**) Immunofluorescence detection of Pdi1-GFP in WT cne1 and Δcne1 *S. cerevisiae* cells treated with MTX for 4 h. The yeast cells were visualized by phase-contrast (DIC) and fluorescent microscopy. (**i**) Quantitative analysis of the immunofluorescence data in (**h**)

anti-cancer chemotherapy (middle panels of Figure 7c).[2,4] Next, we investigated whether intratumoral injection of rec.CRT protein would restore the chemotherapeutic response of ERp57^{low} CT26 cells *in vivo*. The simultaneous treatment of ERp57^{low} CT26 tumors with MTX and exogenous CRT indeed led to elimination of the tumor, provided that the tumors were grown in immunocompetent mice (lower panels in Figure 7c). WT or ERp57^{low} CT26 cells implanted into athymic (*nu/nu*) mice could not be successfully treated with this combination of agents (not shown), indicating the obligate involvement of a T-cell-mediated immune response for successful chemotherapy.

Concluding remarks. We have found that a number of cell lines treated with anthracyclines or UVC light, including CT26 colon cancer cells,[2] MCA 205 fibrosarcoma cells[4] and Lewis

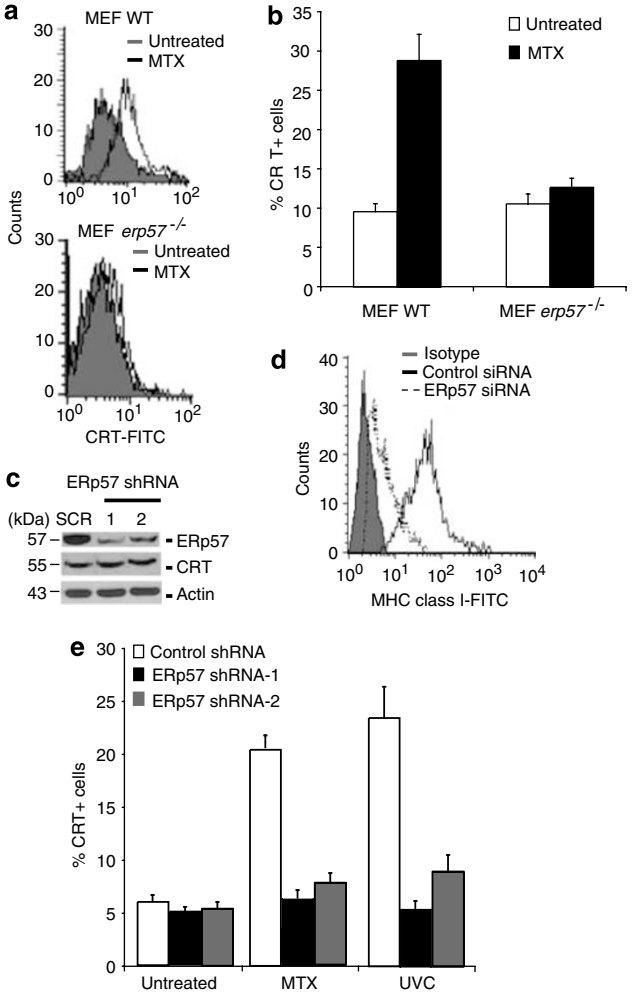

Figure 4 ERp57 is required for the translocation of CRT to the cell surface. (**a**) WT and *erp57*$^{-/-}$ MEF were treated with MTX for 2 h and analyzed for CRT exposure by cytofluorimetric immunodetection. (**b**) Quantitative analysis of cells with surface CRT after incubation of WT and *erp57*$^{-/-}$ MEF with MTX. Data are the means ± S.E.M. of three independent experiments. (**c**) Immunoblot analysis of ERp57 and CRT in CT26 cells stably expressing a scrambled shRNA sequence or two different shRNA sequences specific for ERp57. Actin was used as a loading control. (**d**) Cell surface immunofluorescent detection of MHC class I in control shRNA CT26 and ERp57 shRNA clones. (**e**) Quantitative analysis of control shRNA CT26 and ERp57 shRNA CT26 clones with surface CRT upon treatment with the indicated agents. Data are the means ± S.E.M. of three independent experiments

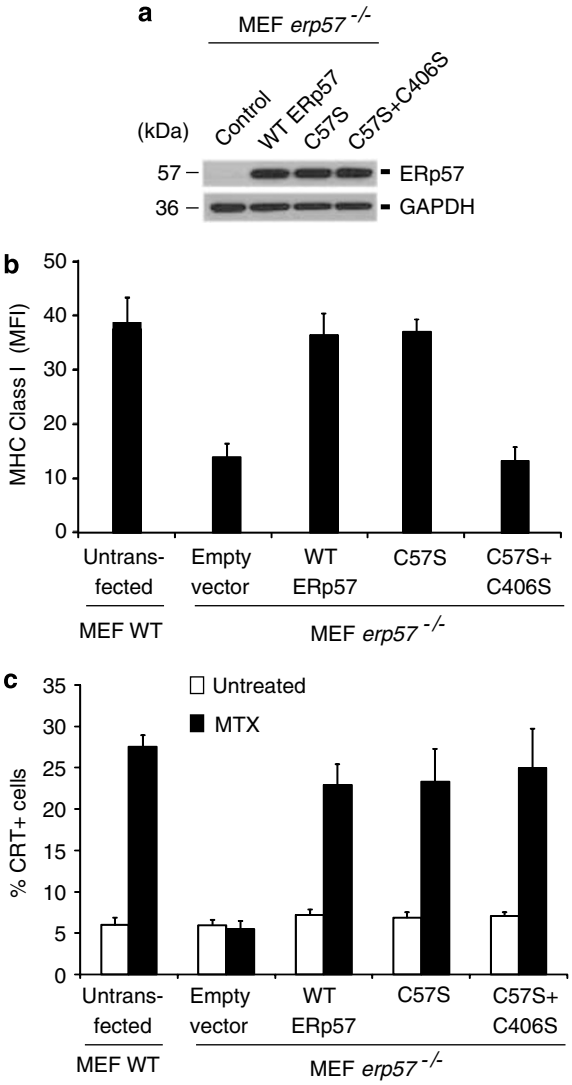

Figure 5 ERp57 isomerase activity is not required for CRT exposure. (**a**) Immunoblot analysis of *erp57*$^{-/-}$ MEF transfected with either an empty vector or the indicated MYC-tagged ERp57 constructs. The expressed ERp57 constructs were visualized with an anti-ERp57 antibody. GAPDH was used as a loading control. (**b**) Quantitative analysis of the mean fluorescence intensity (MFI) of MHC class I on the surface after transfection of *erp57*$^{-/-}$ MEF with the indicated constructs. (**c**) Quantitative analysis of cells with CRT on the surface after transfection of *erp57*$^{-/-}$ MEF with the indicated constructs and treatment with MTX for 2 h. Data are the means ± S.E.M. of three independent experiments

non-small-cell lung cancer cells (unpublished), expose ecto-CRT,[2,4] as well as ecto-ERp57 (present study). Importantly, cytoplasts (enucleated cells) are as efficient in exposing CRT on their surface in response to anthracyclines as are intact cells, indicating that the critical lesion set by anthracyclines is cytoplasmic and does not involve a nuclear DNA damage response.[2] Although the mechanistic details of CRT/ERp57 translocation to the cell surface are unknown, it appears that caspase activation,[1,15] induction of an ER stress response[2] and actin cytoskeleton-dependent transport[16] are involved. Furthermore, as determined here by mutational analyses, the two proteins CRT and ERp57 are transported in a molecular complex that involves direct protein/protein interactions yet does not require the PDI activity of ERp57. Moreover, knockout or knockdown of ERp57 fully inhibits CRT exposure. In contrast, ERp57 is not required for the adsorption of exogenous CRT protein to the cell surface, indicating that CRT alone, in the absence of ERp57, can bind to the cell surface. Indeed, we have been unable to adsorb exogenous ERp57 protein to cells, suggesting that ERp57 binds to the PM in an indirect fashion, via CRT.

Cancer cells subjected to the stable knockdown of ERp57 exhibit reduced immunogenicity *in vivo*, yet are fully susceptible to anthracycline-induced apoptosis and cell killing *in vitro*. This discrepancy can be explained by the fact that anthracycline-mediated anti-cancer therapy relies on two distinct

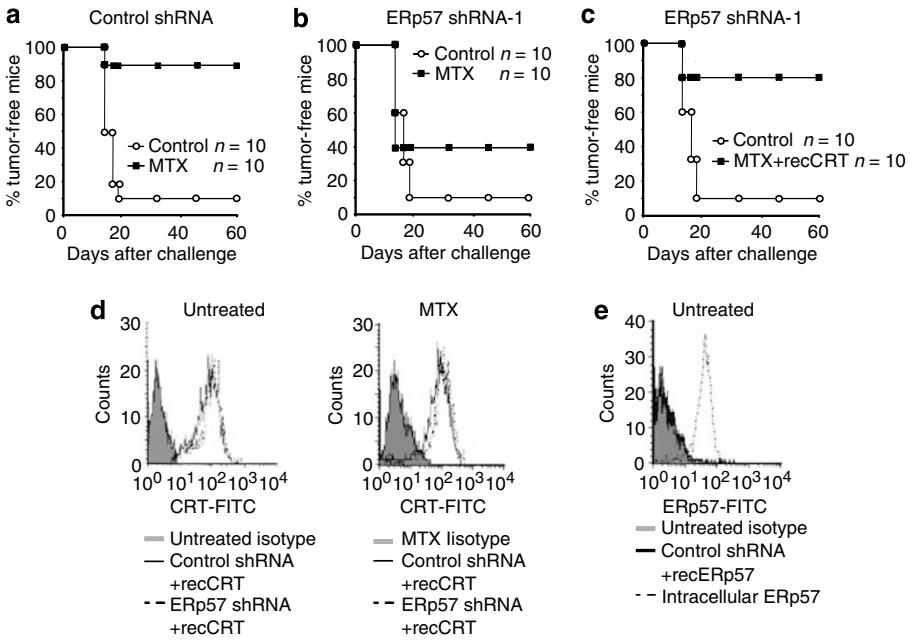

Figure 6 ERp57 is required for MTX-induced immunogenic cell death. (**a**) Mice were injected with PBS (control) or with control shRNA CT26 cells treated with MTX for 4 h. Seven days later, mice were inoculated with live CT26 cells and tumor growth was monitored. (**b**) In an identical setting to (**a**), mice were injected with ERp57 shRNA-1 CT26 cells treated with MTX for 4 h. (**c**) ERp57 shRNA-1 CT26 cells, treated with MTX for 4 h and coated with rec.CRT, were injected into mice 7 days before inoculation with live control CT26 cells. Tumor growth was monitored for the indicated time. (**d**) Control shRNA and ERp57 shRNA-1 cells were treated with MTX for 4 h, coated with rec.CRT followed by quantification of surface levels of CRT by flow cytometry. (**e**) Control shRNA cells were coated with recERp57 followed by quantification of surface and intracellular levels of ERp57 by flow cytometry. These experiments were repeated at least three times, yielding similar results

effects. First, anthracyclines mediate direct anti-tumor effects, which are not influenced by ERp57 expression. Second, anthracyclines can induce immunogenic cell death, causing innate and cognate immune effectors to mount an anti-cancer response and to destroy residual tumor cells. Apparently, ERp57^{low} cells (which cannot expose CRT in response to MTX) fail to stimulate such an anti-cancer immune response unless rec.CRT protein is adsorbed to their surface or rec.CRT is injected into ERp57^{low} tumors. Strikingly, such ERp57^{low} cells (which have low levels of MHC class I *in vitro*) can be efficiently eliminated after co-injection of CRT plus MTX in a setting in which T cells are required for the therapeutic response. This implies that immune effectors can attack other targets in addition to class I (such as class II-restricted tumor antigen, which is well described for CT26 cells[29,30]), that low amounts of MHC class I are sufficient to mediate cytotoxic T-cell responses (note that the class I defect is only partial) or that tumors that express low class I levels *in vitro* acquire MHC class I *in vivo* as a result of local inflammatory responses. Indeed, animals that had been successfully immunized with MTX-treated CT26 cells and protected against CT26 WT cells also rejected CT26 ERp57^{low} cells (T Panaretakis, unpublished data).

Irrespective of these details, it appears that a tumor cell-intrinsic defect in CRT exposure can cause a novel type of anthracycline resistance, due to the inability of tumor cells to elicit an anti-cancer immune response. It will be important to explore the CRT-translocating machinery in more detail and to correlate defects in CRT exposure with therapeutic anthracycline responses at the experimental and clinical levels. Indeed, we found that malignant myeloblasts from some patients with acute myeloid leukemias do manifest an increase in CRT exposure after intravenous injection of anthracyclines *in vivo*, whereas circulating tumor cells from other patients failed to do so.[31] It will be important to correlate the clinical outcome of anti-cancer therapy with CRT exposure in AML as well as in other malignancies.

Materials and Methods

Antibodies and reagents. The rabbit polyclonal (ab2907) and mouse monoclonal (ab22683) antibodies to CRT and the rabbit polyclonal to ERp57 (ab10287) antibodies were from Abcam. For the simultaneous staining of CRT and ERp57 and certain western blots, the chicken anti-CRT antibody (ab61422) from Abcam was used. The mouse anti-actin monoclonal antibody was from AbCys S.A. The H2k^b-FITC was from BD Pharmingen. The anti-GAPDH was from Abcam. Bacitracin was purchased from Sigma-Aldrich and was used at 3 mM, 30 min before treatment with MTX.

Cells, transfection and treatments. CT26 cells were maintained in RPMI 1640 medium and HeLa and WT, *crt*$^{-/-}$ and *erp57*$^{-/-}$ MEF were cultured in Dulbecco's modified Eagle's medium medium (GIBCO). All media were supplemented with heat-inactivated fetal bovine serum (FBS), 10 mM Hepes, 100 U/ml penicillin and 100 μg/ml streptomycin. For transfection of *crt*$^{-/-}$ and *erp57*$^{-/-}$ MEF, cells (1×10^5 cells/well) were seeded into 12-well plates and transfected 24 h later with each expression vector plasmid by using lipofectamine™ 2000 (GIBCO BRL) according to the manufacturer's instructions. CT26 cells were transfected with siRNA heteroduplexes specific for CRT (sense strand: 5′-rCrCrGrCUrGrGrGUrCrGrArAUrCrRrArATT-3′) at a final concentration of 100 nM using HiPerFect (Qiagen). Forty-eight hours after transfection, CT26 cells were assessed for total CRT content by immunoblotting. To restore ecto-CRT, cells were incubated with recCRT, produced in insect cells,[2] at 3 μg/10^6 cells in phosphate-buffered saline (PBS) on ice for 30 min, followed by three washes. For the kinetics of CRT/ERp57 exposure and assessment of cell death, cells were treated for the indicated times and then washed and incubated with fresh, drug-free medium, until they were collected at 20 h from the time of the initial treatment.

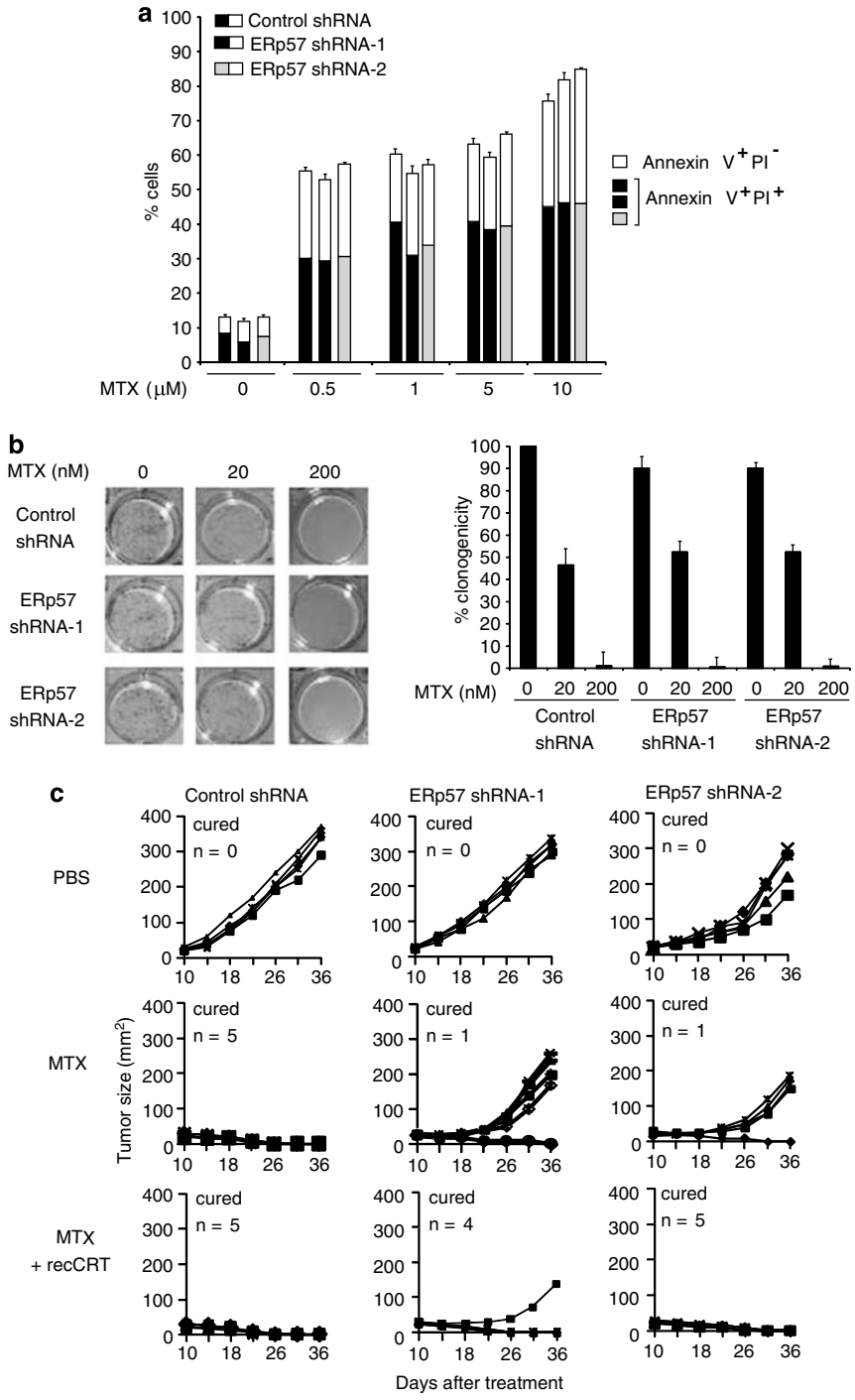

Figure 7 CRT restores deficient chemotherapy responses of ERp57^{low} cells *in vivo*. (**a**) Quantitative analysis of annexin V-FITC and PI staining of control shRNA and ERp57 shRNA CT26 cell clones treated with the indicated concentrations of MTX for 48 h. Results are the means ± S.E.M. of three experiments. (**b**) CT26 cells stably expressing control shRNA, or ERp57 shRNA-1 or shRNA-2 were treated with the indicated concentrations of MTX, washed and plated to determine the frequency of surviving clones. The frequency of clones from untreated control shRNA cells was defined as 100%. (**c**) CT26 tumors from the indicated control and ERp57 shRNA clones were established in mice and when the tumors reached 25–30 mm^2 in size, PBS (upper panels), 1 μM MTX (middle panels) or 1 μM MTX plus 25 μg rec.CRT (lower panels) were injected intratumorally. Tumor size was monitored every 4 days with a caliper. Each treatment group included five mice and was repeated three times with similar results

Plasmid construction. For construction of ERp57 shRNA, self-annealing oligonucleotides containing inverted repeats separated by a spacer sequence and corresponding to nt 521–541 of mouse ERp57 coding sequence were synthesized. The following oligonucleotides were used: sense, 5′-TCGAAGCCAGCAACTTG AGAGATAAGACTCCTGTTATCTCTCAAGTTGCTGGCTTTTTT-3′; antisense, 5′-CTAGAAAAAAGCCAGCAACTTGAGAGATAACAGGAGTCTTATCTCTCAAGTTG CTGGCT-3′ (21 nt target is underlined). This siRNA has previously been used to knock down ERp57.[32] Oligonucleotides were cloned into the pSuppressorRetro

vector (Imgenex, San Diego, CA, USA), which carries the U6 gene promoter and allows expression of shRNA. A scrambled sequence provided by the kit was used as a control. shRNA plasmids were then transfected, along with packaging vectors gag-pol and vsv-g, into HEK293T cells, and retroviral supernatants were concentrated by centrifugation, as described in the manufacturer's instructions.

For generation of isomerase-dead ERp57, site-directed mutagenesis was performed on human ERp57 cDNA (GenBank #U42068) using the QuikChange kit (Stratagene). The C57S and C406S mutations were engineered using the following oligonucleotides, respectively: 5′-TCTTCGCTCCCTGGAGTGGACACTGCAAG-3′ and 5′-GAATTTTATGCCCCTTGGAGTGGTCATTGTAAGAACCT-3′ (codon mutated is underlined). WT, C57S single mutant and C57S/C406S double mutant ERp57 cDNAs were excised with *Eco*RI and cloned into pCMV-Tag3A (Stratagene), downstream and in-frame to a c-myc epitope.

Generation of shRNA stable cell clones. For generation of stable shRNA-expressing cell clones, CT26 cells were infected with retroviral particles carrying the ERp57 or scrambled shRNA plasmids, and several clones were isolated following selection in geneticin (0.1 mg/ml) for 10 days. Knockdown of ERp57 was confirmed by western blotting.

Flow cytometric analysis of CRT and ERp57 on the cell surface. Flow cytometry was used to detect CRT and ERp57 exposure induced by MTX and UVC light. Briefly, 2×10^5 cells were plated in 12-well plates and the day after treated with the indicated agents for 2 h. Cells were collected, washed twice with PBS and fixed with 0.25% paraformaldehyde (PFA) in PBS for 5 min. After washing again twice in cold PBS, cells were incubated for 30 min with primary antibody, diluted in cold blocking buffer (2% FBS in PBS), followed by washing and incubation with the FITC-conjugated monoclonal or polyclonal secondary antibody diluted 1 : 500 in blocking buffer (30 min). Each sample was then analyzed by FACScan (Becton Dickinson) to identify cell-surface CRT and ERp57. Isotype-matched IgG antibodies were used as a control, and the fluorescent intensity of stained cells was gated on PI- or 4′,6-diamidino-2-phenylindole (DAPI)-negative cells.

Immunofluorescence. For surface staining, cells were cultured on 13 mm round glass coverslips as described above. After treatment, cells were placed on ice, washed twice with PBS and fixed with 0.25% PFA in PBS for 5 min. Cells were then washed twice in PBS and primary antibody, diluted in cold blocking buffer, was added for 30 min. After three washes in cold PBS, cells were incubated for 30 min with the appropriate secondary antibody diluted 1 : 500 in cold blocking buffer. Cells were washed with PBS and mounted on slides with the mounting medium including DAPI from Vectashield. For intracellular staining, cells were washed with PBS, fixed with 4% PFA for 20 min, permeabilized with 0.1% Triton X-100 for 10 min, rinsed three times with PBS and nonspecific binding sites were blocked with 10% FBS in PBS for 30 min. Primary antibody was added for 1 h. Subsequently, cells were washed three times with PBS and incubated for 30 min in Alexa Fluor FITC or 568-conjugated secondary antibodies (1 : 1000; Molecular Probes). Lipid rafts were detected with cholera toxin subunit B conjugated to Alexa 488 (Invitrogen), following the manufacturer's instruction, before fixation and CRT staining. Fluorescence microscopic assessment was performed with a Leica confocal microscope (AF6000).

Western blot analyses. Cells were collected and homogenized in RIPA lysis buffer (10 mM Tris, pH 7.2, 150 mM NaCl, 1% deoxycholate, 1% Triton X-100, 0.1% SDS, 5 mM EDTA) containing complete protease inhibitor cocktail (Roche Diagnostics, Meylan, France). After 1 h on ice, samples were sonicated and protein quantification was carried out using a Bio-Rad protein assay. Equal amounts of soluble proteins (15–25 g) were denatured by boiling and resolved by sodium dodecyl sulfate-polyacrylamide gel electrophoresis (SDS-PAGE) and transferred to a nitrocellulose membrane. After blocking in 5% non-fat dry milk in PBS for 1 h and probing with a specific primary antibody and a horseradish peroxidase-conjugated secondary antibody, the protein bands were detected by chemiluminescence (Supersignal, Pierce) and X-ray film exposure (Kodak). Protein loading was normalized by using anti-GAPDH or anti-actin antibodies.

Assessment of apoptosis. Redistribution of PM phosphatidylserine is a marker of apoptosis and was assessed by annexin fluorescein isothiocyanate (MACS, Miltenyi Biotech).[33,34] Briefly, 2×10^5 cells per sample were collected, washed in PBS, pelleted and resuspended in incubation buffer (10 mM Hepes/NaOH, pH 7.4, 140 mM NaCl, 5 mM $CaCl_2$) containing 1% annexin V and PI. Samples were kept in the dark and incubated for 15 min before the addition of another 400 l of incubation buffer and subsequent analysis on a fluorescence-activated cell sorter Calibur flow cytometer (Becton Dickinson) using Cell Quest software.

Biotinylation and immunoprecipitation of cell surface proteins. Biotinylation and recovery of cell surface proteins were performed with a method adapted from Gottardi *et al.*[35] and Hanwell *et al.*[36] Briefly, 20×10^6 HeLa cells grown on 75 cm^2 flask were placed on ice and washed three times with ice-cold PBS-Ca^{2+}-Mg^{2+} (PBS with 0.1 mM $CaCl_2$ and 1 mM $MgCl_2$). Membrane proteins were then biotinylated by a 30-min incubation at 4°C with 1.25 mg/ml NHS-SS-biotin (Pierce) freshly diluted into biotinylation buffer (10 mM triethanolamine, 2 mM $CaCl_2$, 150 mM NaCl, pH 7.5) with gentle agitation. CT26 cells were rinsed with PBS-Ca^{2+}-Mg^{2+} + glycine (100 mM) and washed in this buffer for 20 min at 4°C to quench unreacted biotin. The cells were then rinsed twice with PBS-Ca^{2+}-Mg^{2+}, scraped in cold PBS and pelleted at 2000 r.p.m. at 4°C. The pellets were solubilized for 45 min in 200 μl of lysis buffer (1% Triton X-100, 150 mM NaCl, 5 mM EDTA, 50 mM Tris, pH 7.5) containing protease inhibitors. The lysates were clarified by centrifugation at 14 000 × *g* for 10 min at 4°C and the supernatants were incubated overnight with anti-CRT (mouse monoclonal) antibody or an isotype-matched control antibody (mouse IgG2a). The samples were then incubated overnight with packed streptavidin-agarose beads to recover the biotinylated proteins. The beads were then pelleted by centrifugation and aliquots of supernatants were taken to represent the unbound, intracellular pool of proteins. Biotinylated proteins were eluted from the beads by heating to 100°C for 5 min in SDS-PAGE sample buffer before loading onto a 4–12% Bis-Tris gradient gel (Invitrogen). The rabbit polyclonal ERp57 antibody was used to detect CRT–ERp57 interaction by immunoblotting. To ensure the absence of leakage of biotin into the cells, we verified the absence of the intracellular protein actin in biotinylated extracts.

Two-dimensional gel electrophoresis analysis and protein identification by mass spectrometry. Purified proteins precipitated using the Ettan 2-D clean up kit (GE Healthcare) were subsequently resuspended in urea buffer (7 M urea, 2 M thiourea, 2% Chaps, 1% sulfobetaine SB3-10, 1% amidosulfobetaine ASB14, 50 mM dithiothreitol). For the first dimension of protein separation, isoelectric focusing was performed using 18-cm immobilized nonlinear pH gradient strips (pH 3–10; GE Healthcare) on an IPGphor II electrophoresis unit (GE Healthcare). Proteins (100 μg) were loaded by in-gel rehydratation for 9 h, using low voltage (30 V), and then run using a program in which the voltage was set for 1 h at 100 V, 2 h at 200 V, 1 h at 500 V, 1 h at 1000 V, 2 h at 1000–8000 V and 4 h at 8000 V. Before the second-dimension electrophoresis, IPG gel strips were equilibrated for 10 min at room temperature in 1% dithiothreitol to reduce the proteins and sulfhydryl groups were subsequently derivatized using 4% iodoacetamide (both solutions were prepared in 50 mM Tris (pH 8.8)–6 M urea–30% glycerol–2% SDS–2% bromophenol blue). Strips were transferred to 1.0-mm-thick 10% (wt/vol) polyacrylamide gels (20 by 20 cm) and the second-dimension gels were run at 50 μA for 6 h. Gels were stained with Sypro Ruby (Bio-Rad) and visualized using a Typhoon 9200 scanner (GE Healthcare). The Investigator HT Analyzer (Genomic Solutions Inc.) was used for matching and analysis of visualized protein spots among differential gels. Background subtraction was used to normalize the intensity value representing the amount of protein per spot.

Differentially expressed spots were excised from the gels with an automatic spot picker (Investigator ProPic, Genomic Solutions Inc.), placed in Eppendorf tubes and destained by washing for 5 min with 50 μl of 0.1 M NH_4HCO_3. Then 50 μl of 100% acetonitrile was added and incubated for another 5 min. The liquid was discarded, the washing steps were repeated one more time and gel plugs were shrunk by the addition of pure acetonitrile. The dried gel pieces were re-swollen with 4.0 ng/μl trypsin (Promega, Madison, WI, USA) in 50 mM NH_4HCO_3 and digested overnight at 37°C. Peptides were concentrated with ZipTip®μC18 pipette tips. Co-elution was performed directly onto a MALDI target with 1 μl of α-cyano-4-hydroxycinnamic acid matrix (5 μg/ml in 50% acetonitrile, 0.1% TFA). MALDI-MS and MALDI-MS/MS were performed on an Applied Biosystems 4700 Proteomics Analyzer with TOF/TOF ion optics. Spectra were acquired in the positive MS reflector mode and calibrated either externally using five peaks of standard (ABI4700 Calibration Mixture) or internally using porcine trypsin autolysis peptide peaks (842.51, 1045.56 and 2211.10 $[M+H]^+$ ions). Mass spectra were obtained from each sample spot by 30 sub-spectra accumulation (each consisting of 50 laser shots) in a 750–4000 mass range. Five best signal-to-noise peaks of each spectrum were selected for MS/MS analysis. For MS/MS spectra, the collision energy was 1 keV and the collision gas was air.[37]

MS and MS/MS data were interpreted using the GPS Explorer software (version 2.1, Applied Biosystems), which acts as an interface between the Oracle database containing raw spectra and a local copy of the MASCOT search engine (version 1.8). Peptide mass fingerprints obtained from MS analysis were used for protein identification in Swiss Prot non-redundant database. All peptide mass values are considered monoisotopic and mass tolerance was set at <50 p.p.m. Trypsin was used as the digestion enzyme, one missed cleavage site was allowed, methionine was assumed to be partially oxidized and serine, threonine and tyrosine were partially phosphorylated. Mascot (Matrix Science) scores greater than 71 were considered to be significant ($P<0.005$). For MS/MS analysis, all peaks with a signal-to-noise ratio greater than 5 were searched against the Swiss Prot database using the same modifications as the MS database. Fragment tolerance less than 0.3 Da was considered.

Yeast strains and growth conditions. The strains (ATCC201388 *MAT**a** his31 leu2Δ0 met15Δ0 ura3Δ0*) with GFP-tagged Cne1p and Pdi1p used for microscopic studies were obtained from Invitrogen. For co-localization studies, the strains BY4741 (*MAT**a**his3Δ1 leu2Δ0 met15Δ0 ura3Δ0*) WT and BY4742 (*MAT**a**; his3Δ1 leu2Δ0 lys2Δ0 ura3Δ0*) from the Euroscarf strain collection were used. Cne1p in strain BY4741 was tagged with a GFP tag and Pdi1p in strain BY4742 was tagged with a YFP tag. All strains were grown on SC medium containing 0.17% yeast nitrogen base (Difco), 0.5% $(NH_4)_2SO_4$ and 30 mg/l of all amino acids (except 80 mg/l histidine and 200 mg/l leucine), 30 mg/l adenine and 320 mg/l uracil with 2% glucose as the carbon source. Strains were grown at 28°C.

The strains (ATCC201388 *MAT**a** his31 leu2Δ0 met15Δ0 ura3Δ0*) with GFP-tagged Cne1p and Pdi1p were used for the generation of several knockout strains. Knockouts were constructed according to Gueldener *et al.*[38] using pUG72 as template for the *URA3* disruption cassette.

The proteins Cne1p and Pdi1p in the strains BY4741 and BY4742 were tagged by either eGFP or YFP. The tagging was performed according to Sheff and Thorn,[39] using the optimized set of GFP cassettes purchased from Euroscarf (pKT209 for GFP tagging and pKT90 for YFP tagging). The strain BY4741 with the C-terminally GFP-tagged Cne1p was mated with BY4742 harboring the C-terminally YFP-tagged Pdi1p. After sporulation, tetrads were dissected using a micromanipulator (Singer Instruments) and spores expressing both Cne1p-GFP and Pdi1p-YFP were studied by microscopy. For this, cells were grown at 28°C in synthetic complete medium and treated with 10 μM of MTX for 4 h. After different periods of incubation in the presence of the drug, cells were viewed by fluorescence microscopy with the use of a small-band eGFP filter or YFP filters (Zeiss) on a Zeiss Axioskop microscope.

Clonogenic assays. CT26 cells (800 cells/well) were seeded in duplicate or triplicate into six-well plates. Once the cells were attached, they were treated with 20 and 200 nM of MTX for 24 h, followed by replacement of the medium with new, drug-free medium. Cells were cultured for up to 14 days. Colonies were fixed and stained with crystal violet. All colonies of 50 or more cells were then counted.

Anti-tumor vaccination and assessment of tumor growth *in vivo*. All animals were maintained in specific pathogen-free conditions, and all experiments followed the Federation of European Laboratory Animal Science Association guidelines. All animal experiments were approved by the Ethical Committee of Institut Gustave Roussy (IGR). 3×10^6 CT26 cells untreated or treated with MTX for 4 h were inoculated subcutaneously in 200 μl PBS into the lower flank of 6-week-old female BALB/c mice (Janvier), whereas 5×10^5 untreated control cells were inoculated into the contralateral flank.[1] For the tumorigenicity assay, 3×10^6 treated or untreated CT26 cells were injected subcutaneously into *nu/nu* mice (IGR animal facility). Tumors of the control side were evaluated weekly using a caliper. Animals bearing tumors in excess of 20–25% of the body mass were killed. In a series of experiments, BALB/c (WT or *nu/nu*) carrying palpable CT26 tumors (implanted 10 days before by injection of 10^6 tumor cells) received a single intratumoral injection of PBS or 100 μl PBS containing the same concentration of MTX as that used *in vitro* or 100 μl PBS containing MTX and rec.CRT (15 μg). The size of tumors was evaluated every 4 days using calipers. None of these treatments caused macroscopic necrosis.

Acknowledgements. We thank Dr Marek Michalak for the WT and *crt*$^{-/-}$ MEF and the CRT constructs. We thank Dr Natalio Garbi for the WT and *erp57*$^{-/-}$ MEF. GK is supported by the Ligue Nationale contre le Cancer (Equipe labellisée), European Commission (Active p53, Apo-Sys, RIGHT, TransDeath, ChemoRes, DeathTrain), Cancéropôle Ile-de-France, Fondation de France and Fondation pour la Recherche Médicale, TP is supported by the Swedish Research Council (Vetenskapsradet), NJ is supported by NSERC (Canada), AT is supported by Poste d'accueil INSERM and OK is supported by EMBO. K-WF and MD are grateful to Fonds zur Förderung der wissenschaftlichen Forschung (Austria) for grant 'Molecular Enzymology'. FM is grateful to Fonds zur Förderung der wissenschaftlichen Forschung (Austria) for grant S-9304-B05. MP is partially supported by grants from Ministero della Salute and AIRC.

1. Casares N, Pequignot MO, Tesniere A, Ghiringhelli F, Roux S, Chaput N *et al.* Caspase-dependent immunogenicity of doxorubicin-induced tumor cell death. *J Exp Med* 2005; **202**: 1691–1701.
2. Obeid M, Tesniere A, Ghiringhelli F, Fimia GM, Apetoh L, Perfettini JL *et al.* Calreticulin exposure dictates the immunogenicity of cancer cell death. *Nat Med* 2007; **13**: 54–61.
3. Obeid M, Panaretakis T, Joza N, Tufi R, Tesniere A, van Endert P *et al.* Calreticulin exposure is required for the immunogenicity of gamma-irradiation and UVC light-induced apoptosis. *Cell Death Differ* 2007; **14**: 1848–1850.
4. Obeid M, Tesniere A, Panaretakis T, Tufi R, Joza N, van Endert P *et al.* Ecto-calreticulin in immunogenic chemotherapy. *Immunol Rev* 2007; **220**: 22–34.
5. Apetoh L, Ghiringhelli F, Tesniere A, Obeid M, Ortiz C, Criollo A *et al.* Toll-like receptor 4-dependent contribution of the immune system to anticancer chemotherapy and radiotherapy. *Nat Med* 2007; **13**: 1050–1059.
6. Apetoh L, Ghiringhelli F, Tesniere A, Obeid M, Ortiz C, Criollo A *et al.* Toll-like receptor 4-dependent contribution of the immune system to anticancer chemotherapy and radiotherapy. *Nat Med* 2007; **13**: 1050–1059.
7. Zitvogel L, Apetoh L, Ghiringhelli F, Kroemer G. Immunological aspects of cancer chemotherapy. *Nat Rev* 2008; **8**: 59–73.
8. Groenendyk J, Lynch J, Michalak M. Calreticulin, Ca^{2+}, and calcineurin – signaling from the endoplasmic reticulum. *Mol Cells* 2004; **17**: 383–389.
9. Coppolino MG, Woodside MJ, Demaurex N, Grinstein S, St-Arnaud R, Dedhar S. Calreticulin is essential for integrin-mediated calcium signalling and cell adhesion. *Nature* 1997; **386**: 843–847.
10. Kwon MS, Park CS, Choi K, Ahnn J, Kim JI, Eom SH *et al.* Calreticulin couples calcium release and calcium influx in integrin-mediated calcium signaling. *Mol Biol Cell* 2000; **11**: 1433–1443.
11. Oliver JD, Roderick HL, Llewellyn DH, High S. ERp57 functions as a subunit of specific complexes formed with the ER lectins calreticulin and calnexin. *Mol Biol Cell* 1999; **10**: 2573–2582.
12. Silvennoinen L, Myllyharju J, Ruoppolo M, Orru S, Caterino M, Kivirikko KI *et al.* Identification and characterization of structural domains of human ERp57: association with calreticulin requires several domains. *J Biol Chem* 2004; **279**: 13607–13615.
13. Holaska JM, Black BE, Rastinejad F, Paschal BM. Ca^{2+}-dependent nuclear export mediated by calreticulin. *Mol Cell Biol* 2002; **22**: 6286–6297.
14. Michalak M, Burns K, Andrin C, Mesaeli N, Jass GH, Busaan JL *et al.* Endoplasmic reticulum form of calreticulin modulates glucocorticoid-sensitive gene expression. *J Biol Chem* 1996; **271**: 29436–29445.
15. Obeid M, Panaretakis T, Tesniere A, Joza N, Tufi R, Apetoh L *et al.* Leveraging the immune system during chemotherapy: moving calreticulin to the cell surface converts apoptotic death from 'silent' to immunogenic. *Cancer Res* 2007; **67**: 7941–7944.
16. Tufi R, Panaretakis T, Bianchi K, Criollo A, Fazi B, Di Sano F *et al.* Reduction of endoplasmic reticulum Ca(2+) levels favors plasma membrane surface exposure of calreticulin. *Cell Death Differ* 2008; **15**: 274–282.
17. Berwin B, Delneste Y, Lovingood RV, Post SR, Pizzo SV. SREC-I, a type F scavenger receptor, is an endocytic receptor for calreticulin. *J Biol Chem* 2004; **279**: 51250–51257.
18. Gardai SJ, McPhillips KA, Frasch SC, Janssen WJ, Starefeldt A, Murphy-Ullrich JE *et al.* Cell-surface calreticulin initiates clearance of viable or apoptotic cells through trans-activation of LRP on the phagocyte. *Cell* 2005; **123**: 321–334.
19. Duus K, Pagh RT, Holmskov U, Hojrup P, Skov S, Houen G. Interaction of calreticulin with CD40 ligand, TRAIL and Fas ligand. *Scand J Immunol* 2007; **66**: 501–507.
20. Gallego MA, Joseph B, Hemstrom TH, Tamiji S, Mortier L, Kroemer G *et al.* Apoptosis-inducing factor determines the chemoresistance of non-small-cell lung carcinomas. *Oncogene* 2004; **23**: 6282–6291.
21. Garbi N, Hammerling G, Tanaka S. Interaction of ERp57 and tapasin in the generation of MHC class I-peptide complexes. *Curr Opin Immunol* 2007; **19**: 99–105.
22. Hirano N, Shibasaki F, Sakai R, Tanaka T, Nishida J, Yazaki Y *et al.* Molecular cloning of the human glucose-regulated protein ERp57/GRP58, a thiol-dependent reductase. Identification of its secretory form and inducible expression by the oncogenic transformation. *Eur J Biochem/FEBS* 1995; **234**: 336–342.
23. Antoniou AN, Ford S, Alphey M, Osborne A, Elliott T, Powis SJ. The oxidoreductase ERp57 efficiently reduces partially folded in preference to fully folded MHC class I molecules. *EMBO J* 2002; **21**: 2655–2663.
24. Leys CM, Nomura S, LaFleur BJ, Ferrone S, Kaminishi M, Montgomery E *et al.* Expression and prognostic significance of prothymosin-alpha and ERp57 in human gastric cancer. *Surgery* 2007; **141**: 41–50.

25. Turano C, Coppari S, Altieri F, Ferraro A. Proteins of the PDI family: unpredicted non-ER locations and functions. *J Cell Physiol* 2002; **193**: 154–163.
26. Bohring C, Krause E, Habermann B, Krause W. Isolation and identification of sperm membrane antigens recognized by antisperm antibodies, and their possible role in immunological infertility disease. *Mol Hum Reprod* 2001; **7**: 113–118.
27. Gao B, Adhikari R, Howarth M, Nakamura K, Gold MC, Hill AB *et al.* Assembly and antigen-presenting function of MHC class I molecules in cells lacking the ER chaperone calreticulin. *Immunity* 2002; **16**: 99–109.
28. Martin V, Groenendyk J, Steiner SS, Guo L, Dabrowska M, Parker JM *et al.* Identification by mutational analysis of amino acid residues essential in the chaperone function of calreticulin. *J Biol Chem* 2006; **281**: 2338–2346.
29. Mimura Y, Mimura-Kimura Y, Doores K, Golgher D, Davis BG, Dwek RA *et al.* Folding of an MHC class II-restricted tumor antigen controls its antigenicity via MHC-guided processing. *Proc Natl Acad Sci USA* 2007; **104**: 5983–5988.
30. Homma S, Komita H, Sagawa Y, Ohno T, Toda G. Antitumour activity mediated by CD4+ cytotoxic T lymphocytes against MHC class II-negative mouse hepatocellular carcinoma induced by dendritic cell vaccine and interleukin-12. *Immunology* 2005; **115**: 451–461.
31. Chaput N, De Botton S, Obeid M, Apetoh L, Ghiringhelli F, Panaretakis T *et al.* Molecular determinants of immunogenic cell death: surface exposure of calreticulin makes the difference. *J Mol Med (Berlin, Germany)* 2007; **85**: 1069–1076.
32. Zhang Y, Baig E, Williams DB. Functions of ERp57 in the folding and assembly of major histocompatibility complex class I molecules. *J Biol Chem* 2006; **281**: 14622–14631.
33. Zamzami N, El Hamel C, Maisse C, Brenner C, Munoz-Pinedo C, Belzacq AS *et al.* Bid acts on the permeability transition pore complex to induce apoptosis. *Oncogene* 2000; **19**: 6342–6350.
34. Castedo M, Ferri K, Roumier T, Metivier D, Zamzami N, Kroemer G. Quantitation of mitochondrial alterations associated with apoptosis. *J Immunol Methods* 2002; **265**: 39–47.
35. Gottardi CJ, Dunbar LA, Caplan MJ. Biotinylation and assessment of membrane polarity: caveats and methodological concerns. *Am J Physiol* 1995; **268**: F285–F295.
36. Hanwell D, Ishikawa T, Saleki R, Rotin D. Trafficking and cell surface stability of the epithelial Na^+ channel expressed in epithelial Madin–Darby canine kidney cells. *J Biol Chem* 2002; **277**: 9772–9779.
37. Medzihradszky KF, Campbell JM, Baldwin MA, Falick AM, Juhasz P, Vestal ML *et al.* The characteristics of peptide collision-induced dissociation using a high-performance MALDI-TOF/TOF tandem mass spectrometer. *Anal Chem* 2000; **72**: 552–558.
38. Gueldener U, Heinisch J, Koehler GJ, Voss D, Hegemann JH. A second set of loxP marker cassettes for Cre-mediated multiple gene knockouts in budding yeast. *Nucleic Acids Res* 2002; **30**: e23.
39. Sheff MA, Thorn KS. Optimized cassettes for fluorescent protein tagging in *Saccharomyces cerevisiae*. *Yeast (Chichester, England)* 2004; **21**: 661–670.

Supplementary Information accompanies the paper on Cell Death and Differentiation website (http://www.nature.com/cdd)